Korean J. Chem. Eng., 34(4), 1149-1158 (2017)
DOI: 10.1007/s11814-016-0326-9

pISSN: 0256-1115
eISSN: 1975-7220

Liquid-liquid equilibrium and physical properties of aqueous mixtures of poly(vinyl pyrrolidone) with potassium phosphate at different pH: Experiments and modeling

Abbas Rahmani*, Abbas Ali Rostami*, Mohsen Pirdashti*,†, and Poorya Mobalegholeslam**

*Chemical Engineering Department, Faculty of Engineering, Shomal University, Amol, P. O. Box 731, Iran
**Department of Chemical Engineering, Mahshahr Branch, Islamic Azad University, Mahshahr, Iran
(*Received 2 August 2016 • accepted 20 November 2016*)

Abstract–Liquid-liquid equilibrium data for poly vinyl pyrrolidone (PVP) K30+K_2HPO_4+H_2O system were measured at 298.15 K and different pH values (7.54, 8.05, and 9.47). A binodal curve was fitted to the Merchuk equation and the tie line compositions were fitted to both the Othmer-Tobias and Bancroft equations. The refractive indices and densities of several homogeneous binary and ternary solutions used for calibration were also measured within a range of 0-30 mass% of PVP and 0-50 mass% of K_2HPO_4. Then, the viscosities, densities, electrical conductivities, and refractive indices of binary (PVP K30+water; potassium phosphate+water) and ternary (PVP K30+potassium phosphate+water) systems were measured and correlated at different pH values. The density data showed a linear variation of the polymer and salt mass fractions. The viscosity data of PVP K30 solutions were correlated as a function of the mass fractions by using a nonlinear equation. The effects of the tie line lengths on the densities and viscosities of the aqueous two-phase systems were represented. Also, the modified UNIFAC-NRF is used to calculate the phase equilibria of the mention system. The fitted binary interaction parameters of the model were reported.

Keywords: Liquid-liquid Equilibrium Data, Viscosity, Density, Poly Vinyl Pyrrolidone, Potassium Phosphate, Modified UNIFAC-NRF

INTRODUCTION

Aqueous two-phase systems (ATPSs) can be created from a mixture of two polymers or one polymer and a salt in an aqueous medium separated into two phases. This phenomenon is useful in biotechnology for product separations and has also advantages over conventional extraction methods using organic solvents [1]. ATPS is now recognized as a potential technique because of its multiple advantages including biologic compatibility, ease of continuous process, low interfacial tension, short processing time, low material cost, low energy consumption, good resolution, a high yield, a relatively high load capacity, scaling up feasibility, selective extraction, separation of metal ions and efficient procedure for separation of various biological materials such as recombinant proteins and enzymes [2-13]. Although ATPSs have complementary properties, they have not been broadly adopted for either industrial or commercial purposes. This is due to some main reasons, including the lack of knowledge about LLE data, the physical and thermodynamics properties, the mechanisms that operate in dividing the equilibrium of macromolecules, the absence of a comprehensive theory anticipating the experimental trends, and the empirical nature of the method. Therefore, the inadequacy of the knowledge in this field has motivated the researchers to study ATPSs [14,15].

The design, optimization, and scale-up of the processes require the data from the phase diagram, composition and the physical properties of the phase forming in ATPSs. Furthermore, these data are significant part of the model development since they predict the phase partitioning and are highly required for the separation of biomolecule in an industrial process.

Poly vinyl pyrrolidone (PVP) has been recently used as an alternative inexpensive stable biocompatible polymer soluble in water in industrial production, medicine, and pharmacy [16-19] as forming an ATPS with a suitable salt, though poly ethylene glycol (PEG) has been already studied as an important component in two-phase partitioning. So far, only a few experimental studies have been conducted on PVP phase diagrams, LLE data, and physical properties of the aqueous polymer-salt systems despite the importance of PVP aqueous solutions and abilities to form ATPSs, thus arousing researchers' interests nowadays [20-28]. Additionally, using proper mathematic and thermodynamic models helps to prevent doing expensive and time-consuming experimental efforts at different operational conditions.

The thermodynamic models describing the ATPSs are based on three groups: lattice theory, local composition and virial osmotic theory. In the first group, the molecules are supposed to be in a lattice (a room in the form of a rectangle). Moreover, the interaction of the enthalpy of mixing with neighboring molecules determined the enthalpy of mixing molecules [29]. The local composition thermodynamic models describe the ATPSs in the second group. The most well-known members in the thermodynamic models are Wilson [30], NRTL [31] and UNIQUAC [32]. MNRTL-NRF [33], UNIQUAC-NRF [34] and the modified Wilson [35,36] are the newly

†To whom correspondence should be addressed.
E-mail: pirdashti@yahoo.com

developed versions of these models that are more accurate and have been popular in recent years. The third group of thermodynamic models takes a combination of theories into account to calculate the phase behavior of ATPS, using virial osmotic theory by McMillan and Mayer [37], the Hill theory [38], the solution and the VERS model [39], and extension of the Pitzer model [40]. To model and correlate experimental LLE data, the modified UNIFAC-NRF model [41] was applied and the activity coefficients were utilized. To do this, the appropriate binary interaction parameters are needed since this LLE system is highly non-ideal.

Therefore, we aimed at obtaining phase equilibrium data and binodal data and their correlation for an ATPS containing PVP K30+potassium phosphate at the pH values of 7.54, 8.05, and 9.47. Also, an attempt was made to measure and correlate the viscosity, density, electrical conductivity, and refractive index of binary (PVP K30+water; potassium phosphate+water) and ternary (PVP K30+potassium phosphate+water) systems, as well as the top and bottom phases of the two-phase system. Finally, the modified UNIFAC-NRF model was applied to model the LLE. The modeling involved the use of activity coefficients and the use of appropriate binary interaction parameters were necessary because this LLE system is strongly non-ideal. This model was applied successfully to correlate the experimental LLE data.

EXPERIMENTAL EVALUATION

1. Materials

PVP K30 with a mass average of 40,000 $gmol^{-1}$, potassium phosphate (anhydrous GR>99% for analysis), sodium hydroxide (NaOH; mass purity>0.99%), and sulfuric acid (95-97% H_2SO_4, GR>95.0% for analysis) were obtained from Merck (Darmstadt, Germany) and used without further purification. Distilled deionized water was used to prepare the solutions. All the other materials were of analytical grades.

2. Apparatus and Procedure

Using an analytical balance (A&D, Japan, model GF300) with an accuracy of $\pm 10^{-4}$ g, double-distilled deionized water was added to a 10 g suitable mass of individual solution in 15 mL graduated tubes to prepare the binary (PVP K30+water; potassium phosphate+water) and ternary (PVP K30+potassium phosphate+water) systems. The densities, viscosities, electrical conductivities and refractive indices of the solutions were measured after placing the tubes in a thermostatic bath (Memert., Germany, model INE400) so as to achieve a constant temperature of 298.15 K with an uncertainty of 0.05 K. Using an Anton Paar oscillation U-tube densitometer (model: DMA 500) with a precision of $\pm 10^{-4}$ $g \cdot cm^{-3}$, the densities of the pure liquids and their mixtures were measured based on a double-distilled water and air calibration. Moreover, to measure the viscosities of the solutions within a range of 0.5-300 mPa·s at 298.15 K, an Anton Paar Lovis 2,000 M viscometer of various capillary sizes (1.59-1.8 mm) with a precision of up to 0.5% was employed. The viscosity uncertainties were measured to be ±0.001 mPa·s. Also, using a JENWAY instrument (Model: 4510) with an accuracy of 0.01 μS^{-1} mS, the electrical conductivity was measured at 298.15K. Finally, a refractometer of CETI Belgium model with an accuracy of 0.0001 nD was applied to measure the refractive index.

To determine the binodal curves, a titration method was employed. To make the solution turbid, the polymer and salt solutions of particular concentrations were titrated. The mass could determine the mixture composition. Then, appropriate amounts of the salt, water, and polymer were mixed in 15 mL graduated tubes at 298.15 K to prepare 10 g of the feed samples based on the phase composition data obtained from the above experiments. Meanwhile, an appropriate ratio of potassium phosphate, sodium hydroxide, and sulfuric acid was mixed, respectively, to precisely adjust the pH values of the salt solutions using a pH meter (827 pH, Lab, Metrohm, Swiss made). Before the placement of the test tubes in the thermostatic bath of 298.15 K for 2 h, their contents were rigorously vortexed for 5 min. Then, the tubes were centrifuged (Hermle Z206A, Germany) at 6,000 rpm for 5 min to easily separate the top and bottom samples from the resultant nonturbid phases. Following this, the densities, viscosities, electrical conductivity, and refractive indices of both top and bottom phases were measured at 298.15 K. Thus, the average values of the duplicate measurements of all the above data were reported. To measure the polymer and salt concentrations using the refractive indices and conductivities of both phases at 298.15 K, a calibration approach was applied. To this aim, refractive index and conductivity calibration plots were first prepared based on the known phase compositions and then, the measured values were interpolated.

THERMODYNAMIC FRAMEWORK

The modified UNIFAC-NRF [41] is applied to calculate the phase equilibria of PVP (K30)+K_2HPO_4+H_2O systems. The activity coefficient of component i (polymer, ions and water) is given as the sum of two contributions:

$$\ln \gamma_i = \ln \gamma_i^{LR} + \ln \gamma_i^{M\ UNIFAC-NRF} \tag{1}$$

1. Long-range Interaction Contribution

In this research, the Debye-Hückel equation extended by Pitzer [20,42] was employed for the long-range interactions. The activity coefficient of ion, k, in a solution is:

$$\ln \gamma_k^{LR} = A_x \left[\frac{2Z_k^2}{\rho} \ln \left(\frac{1+\rho I_x^{1/2}}{1+\frac{\rho Z_k}{\sqrt{2}}} \right) + \frac{Z_k^2 I_x^{1/2} - 2I_x^{3/2}}{1+\rho I_x^{1/2}} \right] \tag{2}$$

and for a neutral molecule m (polymer and water):

$$\ln \gamma_m^{LR} = \frac{2A_x I_x^{3/2}}{1+\rho I_x^{1/2}} \tag{3}$$

$$A_x = \frac{1}{3} \left(\frac{2\pi N_A}{V_s} \right)^{1/2} \left(\frac{e^2}{4\pi \varepsilon D_s KT} \right)^{3/2} \tag{4}$$

where Z_k is the ion component of k, N_A is Avogadro's number, K is Boltzmann's constant, ε is the vacuum permittivity and e is the electronic charge. The ρ parameter is considered to be 14.9 [43]. The values for V_s (the molar volume), D_s (dielectric constant) and I_x (the ionic strength in the mole fraction) are obtained by Eqs. (6)-(8). V_s and D_s represent the water and polymer, respectively.

$$V_s = \phi_w^o v_w + \phi_p^o v_p \quad (5)$$

$$D_s = \phi_w^o D_w + \phi_p^o D_p \quad (6)$$

$$I_x = 0.5 \Sigma X_k Z_k^2 \quad (7)$$

The value considered for the dielectric constant D_w is 78.34 and for D_p is 2.2, according to the method proposed by van Krevelen and Hoftyzer [44]. ϕ^o determines the salt-free segment fraction of nonionic species (polymer and water) and is calculated as follows:

$$\phi_p^o = \frac{n_p}{n_w V_w + n_p V_p} \quad (8)$$

$$\phi_w^o = \frac{n_w}{n_w V_w + n_p V_p} \quad (9)$$

2. Short Range Interaction Contribution

2-1. Modified UNIFAC-NRF Model

In the UNICAF-NRF model, the activity coefficient of component i is obtained as:

$$\ln \gamma_i^{M\ UNIFAC-NRF} = \ln \gamma_i^C + \ln \gamma_i^R \quad (10)$$

In Eq. (10), the first part stands for the combinatorial and the second one for the residual part. In this research, the Freed-FV combinatorial model was applied to calculate the combinatorial activity coefficient [44,45]. The activity coefficients of the components were calculated according to the following equation:

$$\ln \gamma_i^C = \ln\left(\frac{\varphi_i^{FV}}{x_i}\right) + 1 - \left(\frac{\varphi_i^{FV}}{x_i}\right) + f_i^{Freed-FV} \quad (11)$$

$$f_i^{Freed-FV} = R_i^{FV}[\Sigma_j \beta_{ji}^{FV} \varphi_j^{FV}(1-\varphi_j^{FV}) - 0.5\Sigma_{j\neq i}\Sigma_{k\neq i}\beta_{jk}^{FV}\varphi_j^{FV}\varphi_k^{FV}] \quad (12)$$

$$\beta_{ji}^{FV} = \alpha_{ji}\left(\frac{1}{R_j^{FV}} - \frac{1}{R_i^{FV}}\right) \quad (13)$$

$$\varphi_i^{FV} = \frac{x_i v_i^{FV}}{\Sigma_j x_j v_j^{FV}} \quad (14)$$

where α_{ji} is the non-random factor which is equal to 0.2, R_j^{FV} is the ratio of v_j^{FV} to v_i^{FV}, whereas v_i^{FV} is the smallest solvent molecule in the aqueous two phase system [46]. v_i^{FV} is the free volume expressed as:

$$v_i^{FV} = v_i - v_i^{vdW} \quad (15)$$

where v_i is the molar liquid volume of component i, while v_i^{vdW} represents the van der Waals volume ($cm^3 \cdot mol^{-1}$) calculated with Eq. (16) [46]:

$$v_i = (0.3 + 4.5\times10^{-4}T)v_i^{vdW} \quad (16)$$

$$v_i^{vdW} = 15.17 R_i \quad (17)$$

and R_i is the volume parameter of group or molecule i. The residual part of the activity coefficient is defined as [34]:

$$\ln \gamma_i^R = \Sigma v_k^{(i)}[\ln \Gamma_k - \ln \Gamma_k^{(i)}] \quad (18)$$

In Eq. (33), $v_k^{(i)}$ describes the number of group k in molecule i and $\ln \Gamma_k^{(i)}$ refers to the activity coefficient of group k in pure solution of molecule i.

$$\ln \Gamma_k = Q_k\left[1 + \ln \xi_{kk} - \sum_{j=1} \Theta_j \xi_{kj} + (1-\Theta_k)\times\sum_{j\neq k}\Theta_j \ln\frac{\xi_{kj}\xi_{jk}}{\xi_{kk}\xi_{jj}} - \frac{1}{2}\sum_{l\neq k}\sum_{\substack{m\neq k \\ m\neq l}}\Theta_l\Theta_m \ln\frac{\xi_{ml}\xi_{lm}}{\xi_{mm}\xi_{ll}}\right] \quad (19)$$

The surface area fraction of group i (Θ_i) is calculated below, where X_k is the relative surface area parameter and Q_k is the mole fraction of group k:

$$\Theta_i = \frac{X_i Q_i}{\Sigma_k X_k Q_k} \quad (20)$$

$$\xi_{ij} = \psi_{ij}\xi_{jj} \quad (21)$$

$$\xi_{kk} = \frac{1}{\Sigma_{\substack{k\neq j \\ for(ion)}}\Theta_j \psi_{ik}} \quad (22)$$

$$\psi_{ij} = \exp\left(-\frac{a_{ij}}{T}\right) \quad (23)$$

where a_{ij} is the variable interaction parameter, ξ_{ij} is the non-random factor of group i which surrounds the central group j.

In this study, to evaluate the activity coefficient of PVP (K30)+

Table 1. Density, ρ, viscosity, η, refractive index, n_D, and electrical conductivity, k, for the PVP K30 (p)+water system at 298.15 K and 0.1 MPa at various mass fractions of PVP (K30), w_P

w_P	ρ (±0.0001)/ kg·m^{-3}	η/ mPa·s	n_D (±0.0001)	k (±0.01)/ μS·cm^{-1}
0.00	0.9970	0.894±0.001	1.3327	500.00
0.05	1.0067	2.296±0.001	1.3402	449.21
0.10	1.0174	5.089±0.001	1.3493	432.23
0.15	1.0270	9.425±0.001	1.3581	408.41
0.20	1.0397	18.05±0.01	1.3664	379.31
0.30	1.0621	66.80±0.01	1.3852	331.12

Standard uncertainties: u(wi)=0.001; u(P)=5 kPa; u(T)=0.05 K

Table 2. Density, ρ, viscosity, η, refractive index, n_D, and electrical conductivity, k, for the potassium phosphate+water system at 298.15 K and 0.1 MPa and different pH values (7.54, 8.05, and 9.47) at various mass fractions of salt, w_s

w_s	ρ (±0.0001)/ kg·m^{-3}	η (±0.001)/ mPa·s	n_D (±0.0001)	k/ mS·cm^{-1}
0.00	0.9970	0.894	1.3327	0.00±0.01
0.02	1.0132	0.879	1.3349	25.4±0.1
0.04	1.0294	0.923	1.3372	44.3±0.1
0.06	1.0468	0.967	1.3404	64.0±0.1
0.08	1.0611	1.008	1.3430	83.3±1
0.10	1.0837	1.082	1.3453	100±1
0.20	1.1691	1.409	1.3594	173±1
0.30	1.2744	2.840	1.3738	224±1
0.40	1.3661	4.648	1.3866	249±1
0.50	1.5096	7.633	1.4014	251±1

Standard uncertainties: u(wi)=0.001; u(P)=5 kPa; u(T)=0.05 K

K_2HPO_4+H_2O system, we assumed that PVP (K30) is distributed to two functional groups, the middle (C_4H_7NO) and the end ($CHCH_2$). However, the salt K_2HPO_4 is divided into ionic groups and water is supposed to be a separate group.

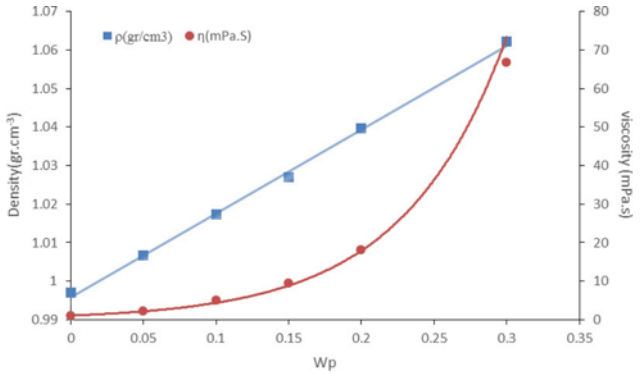

Fig. 1. Density, ρ, and viscosity, η, of the binary PVP K30+H_2O system at 298.15 K as a function of the PVP K30 mass fraction (w_P). The solid curves represent an empirical model.

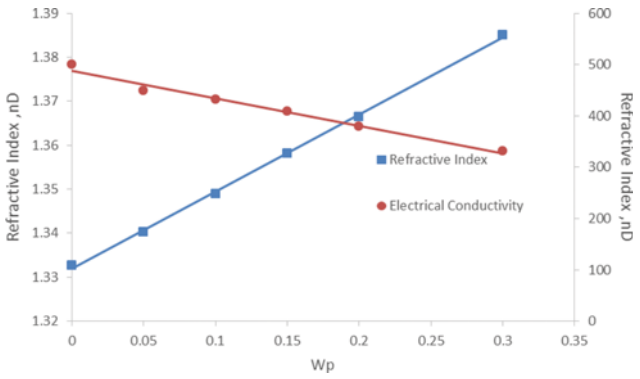

Fig. 2. Refractive index, n_D, and electrical conductivity, k, of the binary PVP K30+H_2O system at 298.15 K and 0.1 MPa as a function of the PVP K30 mass fraction (w_P). The solid curves represent an empirical model.

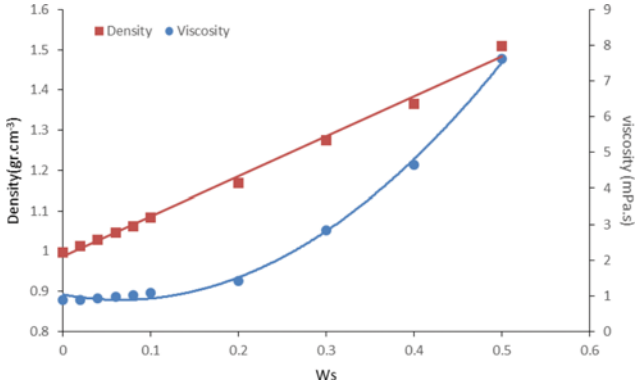

Fig. 3. Density, ρ, and viscosity, η, of the binary potassium phosphate+H_2O system at 298.15 K and 0.1 MPa as a function of the salt mass fraction (w_s). The solid curves represent an empirical model.

RESULTS AND DISCUSSION

1. Physical Properties of Binary and Ternary System

The viscosities, densities, electrical conductivities, and refractive indices of the aqueous solutions of PVP K30+water and potassium phosphate+water at 298.15 K are given in Tables 1 and 2.

As shown in Fig. 1, linear and nonlinear enhancements of the density and viscosity data are caused by increased PVP (K30) mass fraction and as shown in Fig. 3, the same effects were also found in the potassium phosphate+water system. Furthermore, increased refractive indices of the salt (Fig. 2) and polymer solutions (Fig. 4) were observed to be caused by an increasing concentration. Both changes were obviously discovered to be linear. Also, as shown in

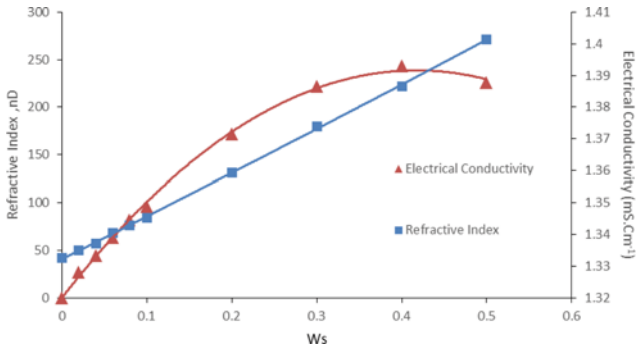

Fig. 4. Refractive index, n_D, and electrical conductivity (k) of the binary potassium phosphate+H_2O system at 298.15 K and different pH values (7.54, 8.05, and 9.47) as a function of the salt mass fraction (w_s). The solid curves represent an empirical model.

Table 3. Density, ρ, viscosity, η, refractive index, n_D, and electrical conductivity, k, for the aqueous single-phase system (PVP K30 (p)+potassium phosphate (s)+water system) at 298.15 K and 0.1 MPa

w_p	w_s	ρ (±0.0001)/ kg·m^{-3}	η/ mPa·s	n_D (±0.0001)	k/ mS·cm^{-1}
0.05	0.02	1.0239	2.390±0.001	1.3440	22.1±0.1
0.10	0.02	1.0323	5.450±0.001	1.3522	20.7±0.1
0.15	0.02	1.0449	11.82±0.01	1.3617	17.0±0.01
0.20	0.02	1.0558	26.87±0.01	1.3700	14.5±0.01
0.25	0.02	1.0654	47.00±0.01	1.3775	12.5±0.01
0.30	0.02	1.0795	77.52±0.01	1.3877	7.5±0.01
0.35	0.02	1.0910	117.7±0.1	1.3959	4.2±0.01
0.05	0.04	1.0397	2.49±0.01	1.3478	40.2±0.01
0.10	0.04	1.0510	6.06±0.001	1.3559	34.8±0.01
0.15	0.04	1.0610	12.43±0.01	1.3639	31.0±0.01
0.20	0.04	1.0736	28.20±0.01	1.3730	28.9±0.01
0.25	0.04	1.0843	47.91±0.01	1.3826	25.6±0.01
0.05	0.06	1.0563	3.093±0.001	1.3502	56.7±0.01
0.10	0.06	1.0665	5.832±0.001	1.3592	49.5±0.01
0.15	0.06	1.0767	13.19±0.01	1.3682	47.0±0.01
0.05	0.08	1.0762	2.744±0.001	1.3539	72.1±0.01
0.10	0.08	1.0867	5.99±0.001	1.3626	65.1±0.01

Standard uncertainties: u(wi)=0.001; u(P)=5 kPa; u(T)=0.05 K

Table 4. Some proposed semi-empirical relations to predict the physical properties of binary systems

Binary system	Equation	Coefficients of equation		R^2
		a	b	
PVP K30+water	$\rho=a+bw_p$	0.9962	0.2133	0.9973
	$\eta=ae^{bw_p}$	0.9974	0.2022	0.9971
	$n_D=a+bw_p$	0.13304	0.1831	0.9994
	$k=a+bw_p$	477.4691	−483.8324	0.9951
Potassium phosphate +water	$\rho=a+bw_s$	0.9833	1.0024	0.9941
	$\eta=ae^{bw_s}$	0.6979	4.9264	0.9956
	$n_D=a+bw_s$	1.3319	0.1435	0.9996
	$k=a(1-b^{-bw_s})$	328.5323	3.6374	0.9998

Table 5. Some proposed semi-empirical relations to predict the physical properties of ternary systems

Equation	Coefficients of equation			R^2
	a	b	c	
$\rho=a+bw_p+cw_s$	0.9935	0.2247	0.8686	0.9984
$\rho=a+be^{w_p}+ce^{w_s}$	−0.0193	0.1866	0.8294	0.9972
$\eta=aw_p^bw_s^c$	1646.2660	2.4461	0.0446	0.9911
$\eta=aw_p^2-bw_s$	693.8808	96.5672	-	0.9763
$\eta=a+be^{w_p}+ce^{w_s}$	−165.2182	165.8336	−9.5696	0.8946
$\eta=a+bw_p+cw_s$	−9.6903	187.5617	16.0501	0.8756
$n_D=a+bw_p+cw_s$	1.3318	0.1734	0.1670	0.9995
$n_D=a(w_p^b+w_s^c)$	0.7181	0.0373	0.0071	0.9061
$n_D=a+blnw_p+clnw_s$	1.4334	0.0246	0.0048	0.8996
$k=a+bw_p+cw_s$	12.3117	−65.5229	741.5878	0.9843
$k=a+blnw_p+clnw_s$	105.9352	−10.2828	28.4170	0.9521
$k=1/(a+be^{w_p}+ce^{w_s})$	0.3229	0.0735	0.3078	0.9005

Table 6. Binodal curve data of the PVP K30+potassium phosphate+water system at 298.15 K and 0.1 MPa at different pH values

pH=7.54		pH=8.05		pH=9.47	
$100w_p$	$100w_s$	$100w_p$	$100w_s$	$100w_p$	$100w_s$
14.34	7.08	14.40	7.00	14.87	6.41
14.05	7.08	14.23	7.07	14.40	6.45
12.49	7.52	13.95	7.09	14.17	6.47
12.27	7.51	13.66	7.27	13.80	6.57
11.95	7.54	13.39	7.27	13.46	6.54
9.41	8.17	9.40	8.06	10.06	7.35
9.18	8.35	9.14	8.15	9.81	7.38
9.01	8.37	8.95	8.17	9.64	7.34
8.74	8.42	8.79	8.22	9.47	7.41
8.56	8.42	8.60	8.24	9.31	7.46
7.13	8.65	7.41	8.44	7.82	7.75
7.02	8.64	7.25	8.51	7.68	7.76
6.92	8.69	7.13	8.54	7.60	7.76
6.80	8.73	7.01	8.55	7.51	7.75
6.71	8.73	6.89	8.56	7.40	7.81
5.65	9.06	5.96	8.79	6.31	8.03
5.49	9.03	5.84	8.80	6.25	8.02
5.42	9.05	5.75	8.81	6.21	8.04
5.35	9.06	5.64	8.83	6.13	8.08
5.30	9.09	5.58	8.84	6.07	8.06
4.09	9.49	5.09	8.90	5.57	8.22
4.02	9.49	5.02	8.92	5.53	8.21
3.98	9.47	4.95	8.99	5.46	8.29
3.90	9.52	4.83	9.07	5.41	8.28
3.79	9.55	4.70	9.02	5.36	8.31
2.85	9.91	4.59	9.10	4.45	8.49
2.01	10.17	4.42	9.12	4.03	8.61
1.51	10.39	3.25	9.40	3.60	8.73
1.06	10.64	1.52	9.96	2.02	9.27
0.26	11.31	0.19	10.79	0.20	10.47

Standard uncertainties: u(wi)=0.002; u(P)=5 kPa; u(T)=0.05 K

Figs. 2 and 3, a high difference was seen between the electrical conductivities of the polymer and salt solutions, respectively. Despite the very low electrical conductivity of the polymer solution, both underwent an increased electrical conductivity by increasing the concentration. Compared to a 224 $mS\cdot cm^{-1}$ change in phosphate salt concentration, a negligible amount of 0.331 $mS\cdot cm^{-1}$ resulted from the polymer solution conductivity when a change of 0-30% (w/w) occurred to the PVP (K30) concentration.

The finding is congruent with most data reported for similar systems in the literature [34,39,41].

The viscosities, densities, electrical conductivities, and refractive indices of the PVP K30+potassium phosphate+water systems are given in Table 3.

Some empirical expressions are proposed in Tables 4-5 for the correlations of the physical properties of the mentioned binary and ternary systems, which are also shown in Figs. 1-4. All our attempts were aimed at reducing the model complexity and increasing its accuracy.

2. Binodal Data

The binodal data obtained from the turbidimetric titrations of PVP (K30)+potassium phosphate+water mixtures at 298.15 K at different pH values (7.54, 8.05, and 9.54) are presented in Table 6.

For the binodal data correlation, the Merchuk equation [47] can be suitably used to reproduce the binodal curves of the investigated systems.

$$w_p = ae^{(bw_s^{0.5}-cw_s^3)} \quad (24)$$

Table 7. Values of parameters of equation 3 for PVP K30+potassium phosphate+water at different pH values

pH	a	b	c	R^2
7.54	0.1201	−1.1720	29.6655	0.9950
8.05	0.1127	−1.0027	30.6277	0.9982
9.47	0.1107	−1.0245	22.7470	0.9967

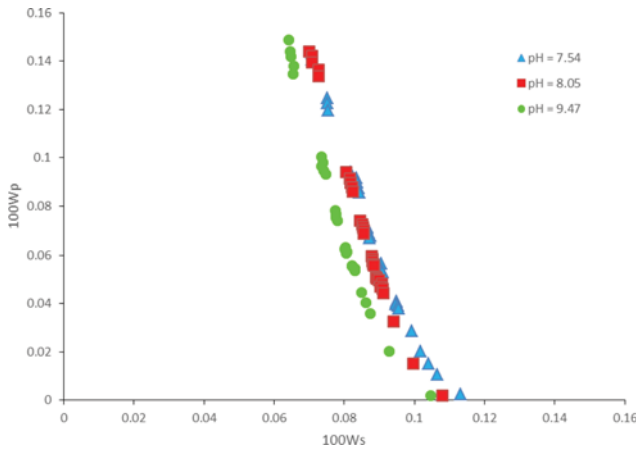

Fig. 5. The experimental and correlated binodal curves of PVP K30+potassium phosphate+water ATPSs at different pH values.

where a, b, and c represent the fitting parameters and w_p and w_s demonstrate the polymer and salt mass fractions, respectively. The binodal data of the above expression were correlated by least-squares regression.

The experimental and correlated binodal curves of the study systems are shown in Fig. 5.

Fig. 5 exhibits pH influence on the binodal curve of the aqueous two-phase PVP K30+potassium phosphate system. This figure shows the binodal downward displacement by the moderate pH augmentation, indicating a need for lower concentrations of the phase polymers for the ATPS formation. Also, a comparable conduct has been depicted in [48-51]. The solute charge, charged species ratio, and binodal location are all functions of pH. A salting-out phenomenon probably caused by the salt's promotability of water structure may occur as the pH rises and the polymer hydrogen-bond interactions consequently weaken. The polymer solubility and reduced hydration might result from the stronger affinity of phosphate salt ions towards water rather than to the polymer. This process may ultimately lead to the polymer exclusion from the rest of the solution [49]. Zafarani-Moattar and Seifi-Aghjekohal (2007) obtained experimentally the LLE data for aqueous polyvinylpyrrolidone (PVP) (average MW=3500)+dipotassium hydrogen phosphate systems at T=(298.15, 308.15 and 318.15) K. They successfully used the Merchuk equation to correlate the experimental binodal data for these systems. In the temperature range considered, the temperature has little effect on the binodal curves for the studied system; the effect of temperature on the binodal curve is only noticeable at higher concentrations of salt. The slopes of all equilibrium tie-lines increase with increasing temperature [25].

Table 8 illustrates the tie line data, equilibrium phase compositions, and physical properties of the top and bottom phases. Four feed solutions containing PVP K30+potassium phosphate+water were applied to perform the experiments at three pH values. The same table presents the experimental results for the feed solutions and the resulting coexistence of the phases.

Likewise, it can be recognized from the data shown in Table 9 that an increment in salt composition at a constant pH causes the PVP concentration enhancement in the top phase. This can be clarified by the salt hydration impact.

Tie-Line Length (TLL) provides an empirical measurement of the compositions of the two phases, which can be calculated by the following equation:

Table 8. Phase composition, tie line data and physical properties of PVP K30+potassium phosphate+water aqueous two phase system at 298.15 K and 0.1 MPa

pH	Total system (%mass)		Top phase				Bottom phase				TLL (%)	−STL (%)
	$100w_p$	$100w_s$	$100w_p$	$100w_s$	ρ (±0.0001)/ kg·m^{-3}	η (±0.01)/ mPa·s	$100w_p$	$100w_s$	ρ (±0.0001)/ kg·m^{-3}	η/ mPa·s		
7.54	14.00	8.00	20.34	6.19	1.0939	41.44	1.58	11.36	1.0957	1.530	18.0	3.63
	10.00	8.00	24.39	5.52	1.0955	50.91	0.47	12.37	1.1027	1.386	22.9	3.49
	12.00	8.00	29.97	3.88	1.0930	53.22	0.27	13.44	1.1088	1.302	26.9	2.99
	12.00	7.50	18.94	6.39	1.0917	29.71	2.36	10.99	1.0941	1.776	15.9	3.60
8.05	10.00	8.50	16.02	6.56	1.0874	20.16	3.26	10.04	1.0890	1.955	13.2	3.66
	12.00	8.50	23.03	5.32	1.0911	45.38	1.41	11.27	1.0948	1.505	20.7	3.63
	12.00	8.00	17.49	6.27	1.0885	12.10	3.99	10.16	1.0898	2.110	12.9	3.47
	14.00	8.00	23.07	5.30	1.0921	45.24	1.67	11.28	1.0946	1.574	20.5	3.58
9.47	8.00	10.00	28.10	4.49	1.0941	92.47	0.65	11.91	1.0994	1.369	26.4	3.70
	10.00	10.00	16.85	6.48	1.0866	20.75	3.98	9.93	1.0878	1.941	13.3	3.73
	12.00	10.00	21.81	5.19	1.0896	48.93	1.98	10.85	1.0909	1.538	19.0	3.50
	12.00	9.00	17.29	6.17	1.0865	22.71	3.27	10.01	1.0874	1.900	13.4	3.65

Standard uncertainties: u(wi)=0.002; u(P)=5 kPa; u(T)=0.05 K

Table 9. Values of the parameters of Eqs. (1) and (2) for PVP K30+potassium phosphate+water at different pH values

pH	k	n	R^2	k_1	r	R^2
7.54	0.0041	3.2175	0.9999	5.7839	0.2722	0.9998
8.05	0.0072	2.9708	1.0000	5.6192	0.2812	0.9924
9.47	0.0279	2.4064	1.0000	4.6495	0.3875	0.9967

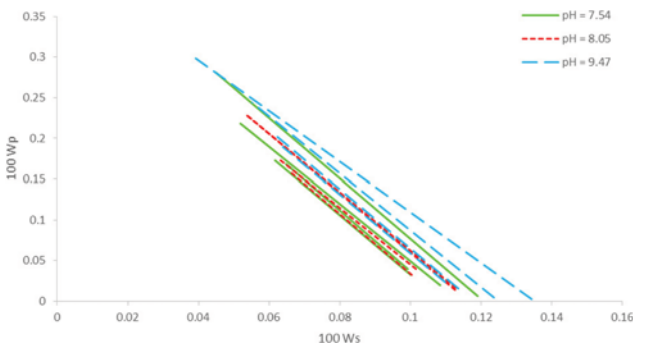

Fig. 6. pH effects on the equilibrium phase compositions and slope and length of tie-lines for the PVP K30+potassium phosphate+H_2O system.

$$TLL=\sqrt{(C_p^{top}-C_p^{bottom})^2+(C_s^{bottom}-C_s^{top})^2} \quad (25)$$

The slope of the tie-line (STL) is given by the ratio of the difference between the polymer (C_P) and salt (C_S) concentrations in the top and bottom phases as presented in Eq. (26):

$$STL=\frac{C_p^{top}-C_p^{bottom}}{C_s^{bottom}-C_s^{top}} \quad (26)$$

In Fig. 6, the effects of pH on the equilibrium phase compositions and the slope and length of the tie lines have been represented for the PVP K30+potassium phosphate+H_2O system. An increase in pH would lead to TLL and STL augmentations in the above system, which might be caused by a reduction in the solution hydrodynamic volume. Likewise, a comparable conduct has been portrayed in [49,51]. A decreased intrinsic viscosity of the polymer solution caused by the pH reduction was reported by Waziri et al. (2003) and Shahbazinasab and Rahimpour (2012). As we know, a decline in pH results in more compact structure of the polymer chains since the intrinsic viscosity of a polymer solution is proportional to its hydrodynamic volume. Additionally, the concentrations of the PVP- and salt-rich phases have been reported to increase and decrease, respectively, as the pH of an aqueous two-phase PVP-salt system enhances [49,52].

The reliability of the measured tie line compositions was ascertained by Othmer-Tobias (Eq. (27)) and Bancroft (Eq. (28)) correlation equations.

$$\left(\frac{1-w_{pt}}{w_{pt}}\right)=k\left(\frac{1-w_{sb}}{w_{sb}}\right)^n \quad (27)$$

$$\left(\frac{w_{wb}}{w_{sb}}\right)=k_1\left(\frac{w_{wt}}{w_{pt}}\right)^r \quad (28)$$

where w_{pt} is the mass fraction of PVP K30 in the top phase, w_{sb} is the mass fraction of K_2HPO_4 in the bottom phase, w_{wb} and w_{wt} are the mass fractions of water in the bottom and top phases, respectively, and k, n, k_1, and r are the parameters. The values of the parameters are given in Table 9.

Also, TLL effects on the densities, dynamic viscosities, and kinematic viscosities of the aqueous two-phase systems were considered. As shown in Figs. 7, 8, and 9, density ($\Delta\rho$) and viscosity ($\Delta\eta$)

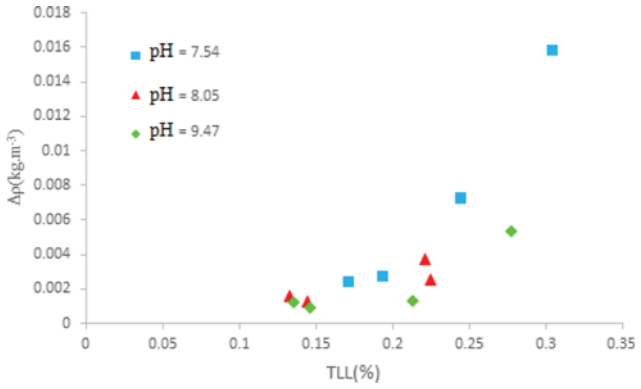

Fig. 7. The relationship between density difference ($\Delta\rho$) and Tie-Line Length (TLL) for the PVP K30+potassium phosphate+water system at different pH values.

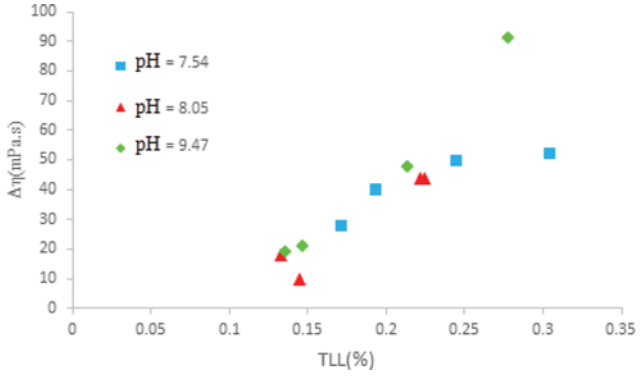

Fig. 8. The relationship between viscosity difference ($\Delta\eta$) and Tie-Line Length (TLL) for the PVP K30+potassium phosphate+water system at different pH values.

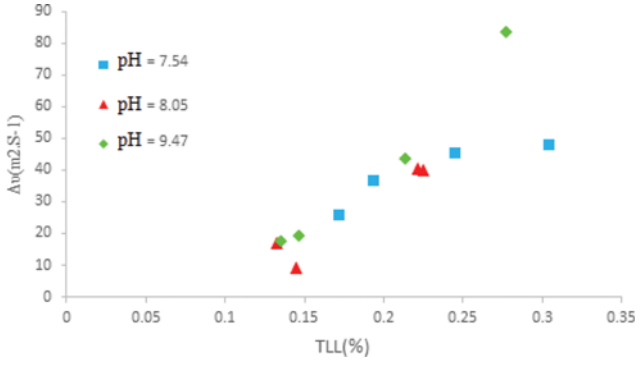

Fig. 9. The relationship between kinematic viscosity difference ($\Delta\nu$) and Tie-Line Length (TLL) for the PVP K30+potassium phosphate+water system at different pH values.

Table 10. The Modified UNIFAC-NRF interaction parameters in the PVP (m: C_4H_7NO and e: $CHCH_2$)+K_2HPO_4 (c: cation and a: anion)+water (w) systems

Systems	a^a_{wm}	a^a_{mw}	a^a_{we}	a^a_{ew}	a^a_{me}	a^a_{em}	ARD%[b]		
PVP+H_2O	−315.71	785.00	−284.00	−165.92	310.84	−771.57	0.11		
	a_{wc}	a_{cw}	a_{wa}	a_{aw}	a_{ca}	a_{ac}	ARD%		
K_2HPO_4+H_2O [53]	−5503.41	1.14	−2326.56	0.50	5338.14	−8810.79	8.39×10^{-3}		
	a_{cm}	a_{mc}	a_{ce}	a_{ec}	a_{am}	a_{ma}	a_{ae}	a_{ea}	Dev%[c]
PVP+K_2HPO_4+H_2O (pH 7.54)	−697.96	897.05	98.41	689.95	−1412.91	12450.42	2042.28	−141.70	0.046
PVP+K_2HPO_4+H_2O (pH 8.05)									0.091
PVP+K_2HPO_4+H_2O (pH 9.47)									0.098

[a]Calculated and reported by Pirdashti et al. [53]

[b]$\mathrm{ARD\%}=\frac{100}{N_p}\Sigma_{n=1}^{NP}\left|\frac{a_{wn}^{cal}-a_{wn}^{exp}}{a_{wn}^{exp}}\right|$ where N_P is the number of experimental data points

[c]$\mathrm{Dev\%}=100\left(\frac{OF}{6N}\right)$; where N is the number of tie-lines

differences between the phases were found to increase and decrease with TLL and pH enhancements, respectively. Similarly, a comparable conduct has been described in [50,51].

3. Thermodynamic Modeling

The modified UNIFAC-NRF model [41] connects the experimental data by minimizing the objective function presented below:

$$OF=\Sigma_p\Sigma_l\Sigma_j\left(w_{p,l,j}^{cal}-w_{p,l,j}^{exp}\right)^2 \quad (29)$$

where $w_{p,l,j}$ is the weight fraction of the j specie in the phase p for *l* tie-line. In Eq. (43), the species j can be a polymer, salt, or solvent molecule and cal denotes the calculated values, whereas the experimental values are shown with exp superscript. The equilibrium condition was used to correlate the liquid-liquid equilibrium records.

$$(x_i\gamma_i)^{top}=(x_i\gamma_i)^{bottom} \quad (30)$$

Apparently, the sum of mole fractions of the three components in every phase should be equal to unity, so the mass balance equation is useful to check the calculated values. Mole fraction calculated values are derived from the stated equations and a suitable model of activity coefficient. In this investigation, the binary interaction parameters, which were published by Pirdashti et al. [41], were used between water and polymer for the modified UNIFAC-NRF model. The interaction parameters of salt and water ions in the modified UNIFAC-NRF model were achieved from the VLE experimental data of K_2HPO_4+H_2O binary system [53].

In this study, the interaction parameters between salt and polymer were obtained from correlation of experimental data with PVP(K30)+potassium phosphate+water in pH=7.54 in the modified UNIFAC-NRF model. The achieved interaction parameters were applied in prediction of PVP(K30)+potassium phosphate+water in pH=8.05 and 9.47. The obtained interaction parameters from experimental data of VLE and LLE models are shown in Table 10. The compar-

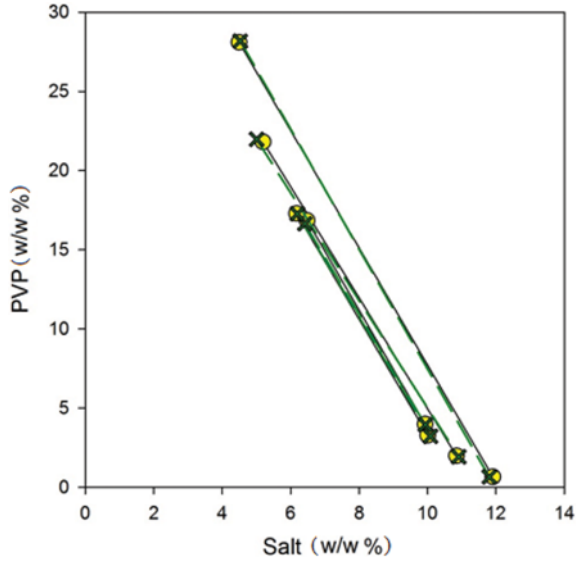

Fig. 10. Comparison of experimental tie-line data with calculated values for PVP K30-K_2HPO_4-H_2O systems at pH=7.54: Experimental data (—○—) and calculated (- -×- -).

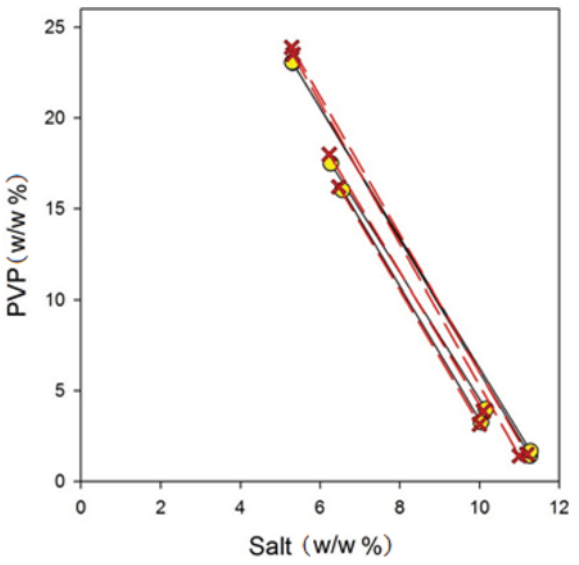

Fig. 11. Comparison of experimental tie-line data with calculated values for PVP K30-K_2HPO_4-H_2O systems at pH=8.05: Experimental data (—○—) and calculated (- -×- -).

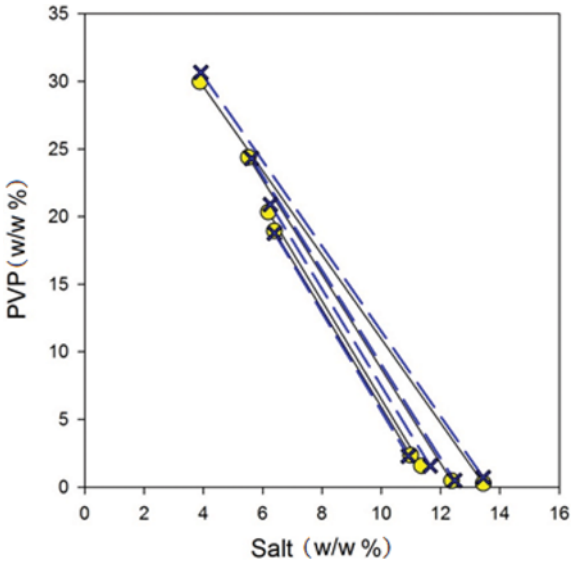

Fig. 12. Comparison of experimental tie-line data with calculated values for PVP K30-K_2HPO_4-H_2O systems at pH=9.47: Experimental data (—○—) and calculated (– ✕ –).

ison of the interaction parameters of the VLE data showed a good agreement with the LLE system in all the mentioned models. To show the reliability of the modified UNIFAC-NRF model, the comparison between the experimental and calculated tie-lines is shown in Figs. 10 to 12 for aqueous PVP K30-K_2HPO_4-H_2O systems at pH=7.54, pH=8.05 and pH=9.47, respectively.

CONCLUSION

New experimental results have been presented for the liquid-liquid equilibrium data of the PVP K30+potassium phosphate+water system at various pH values of 7.54, 8.05, and 9.4 at 298.15 K. The two-phase area was expanded with increasing pH. Also, with pH enhancement, the slope and length of the equilibrium tie-lines were augmented for the mentioned biphasic system. The experimental binodal data were satisfactorily correlated with the Merchuk equation. Moreover, the densities, viscosities, electrical conductivities, and refractive indices of the binary and ternary mixtures of the aqueous two-phase PVP K30+potassium phosphate+water systems were measured and correlated at 298.15 K. Some empirical models were developed to describe the physical properties of binary and ternary systems. The models could precisely reproduce the experimental data.

The data were correlated with the modified UNIFAC-NRF model to determine the activity coefficient. The results of this thermodynamics model are also satisfactory. Furthermore, the obtained binary interaction parameters can be used to predict the phase behavior of the studied ternary system.

REFERENCES

1. R. Hatti-Kaul, *Methods in Biotechnology: Aqueous Two-Phase Systems: Methods and Protocols*, Humana Press Inc., Totowa, NJ (2000).
2. K. Raghavarao, T. Ravganathan, N. Srinivas and R. Barhate, *Clean Technol. Environ. Policy.*, **5**, 136 (2003).
3. E. Espitia-Saloma, P. Vázquez-Villegas, O. Aguilar and M. Rito-Palomares, *Food Bioprod. Process.*, **92**, 101 (2014).
4. F. Luechaua, T. Ch. Ling and A. Lyddiatt, *Biochem. Eng. J.*, **50**, 122 (2010).
5. R. Hu, X. Feng, P. Chen, M. Fu, H. Chen, L. Guo and B.-F. Liu, *J. Chromatogr. A.*, **1218**, 171 (2011).
6. P. A. Rosa, A. M. Azevedo, S. Sommerfeld, W. Bäcker and M. R. Aires-Barros, *Biotechnol. Adv.*, **29**, 559 (2011).
7. K. Naganagouda and V. H. Mulimani, *Process Biochem.*, **43**, 1293 (2008).
8. S. Bradoo, R. K. Saxena and R. Gupta, *Process Biochem.*, **35**, 57 (1999).
9. M. Rito-Palomares, *J. Chromatogr. B: Anal. Technol. Biomed. Life Sci.*, **807**, 3 (2004).
10. J. A. Asenjo and B. A. Andrews, *J. Chromatogr. A.*, **1238**, 1 (2012).
11. G. D. Rodrigues, L. R. de Lemos, L. H. M. da Silva and M. C. H. da Silva, *J. Chromatogr. A.*,**1279**, 13 (2013).
12. L. Bulgariu and D. Bulgariu, *Sep. Purif. Technol.*, **118**, 209 (2013).
13. J. Lan, C.-Y. Yeh, C.-C. Wang, Y.-H. Yang and H.-S. Wu, *J. Biosci. Bioeng.*, **116**, 499 (2013).
14. L. Yan-Min, Y. Yan-Zhao, Z. Xi-Dan and X. Chuan-Bo, *Food Bioprod. Process.*, **88**, 1 (2010).
15. M. V. Rocha and B. B. Nerli, *J. Bio. Macromol.*, **6**, 2 (2013).
16. V. Bühler, *Excipients for Pharmaceuticals-Povidone, Crospovidone and Copovidone*, Springer, Berlin, Heidelberg, New York (2005).
17. M. T. Zafarani-Moattar and A. A. Zaferanloo, *J. Chem. Thermody.*, **41**, 864 (2009).
18. Y. Wang, Y. Wu, L. Ni, J. Han, J. Ma and Y. Hu, *J. Chem. Eng. Data*, **57**, 3128 (2012).
19. M. T. Zafarani-Moattar, N. Karimi and B. Asadzadeh, *J. Mol. Liq.*, **211**, 767 (2015).
20. M. T. Zafarani-Moattar and R. Sadeghi, *Fluid Phase Equilib.*, **203**, 177 (2002).
21. M. T. Zafarani-Moattar and R. Sadeghi, *Fluid Phase Equilib.*, **238**, 129 (2005).
22. A. Salabat, M. A. Moghadasi, P. Zalaghi and R. Sadeghi, *J. Chem. Thermodyn.*, **38**, 1479 (2006).
23. R. Sadeghi, *CALPHAD*, **30**, 53 (2006).
24. R. Sadeghi, H. R. Rafiei and M. Motamedi, *Thermochim. Acta.*, **451**, 163 (2006).
25. M. T. Zafarani-Moattar and P. Seifi-Aghjekohal, *CALPHAD*, **315**, 53 (2007).
26. N. Fedicheva, L. Ninni and G. Maurer, *J. Chem. Eng. Data*, **52**, 1858 (2007).
27. M. Foroutan and M. Zarrabi, *Fluid Phase Equilib.*, **266**, 164 (2008).
28. B. Mokhtarani, H. R. Mortaheb, M. Mafi and M. H. Amini, *J. Chromatogr. B.*, **879**, 721 (2011).
29. J. A. Baskir, T. A. Hatton and U. W. Suter, *J. Phys. Chem.*, **93**, 2111 (1989).
30. H. Renon and J. M. Prausnitz, *AIChE J.*, **14**, 135 (1968).
31. D. S. Abrams and J. M. Prausnitz, *AIChE J.*, **21**, 116 (1975).
32. G. M. Wilson, *J. Am. Chem. Soc.*, **86**, 127 (1964).
33. A. Haghtalab and M. Joda, *Fluid Phase Equilib.*, **278**, 20 (2009).
34. A. Haghtalab and B. Mokhtarani, *Fluid Phase Equilib.*, **215**, 151

(2004).
35. X. Xu, P. P. Madeira, J. A. Teixeira and E. A. Macedo, *Fluid Phase Equilib.*, **213**, 53 (2003).
36. R. Sadeghi, *J. Chem. Thermodyn.*, **37**, 55 (2005).
37. W. G. McMillan and J. E. Mayer, *J. Chem. Phys.*, **13**, 276 (1945).
38. T. L. Hill, *J. Chem. Phys.*, **30**, 93 (1959).
39. A. Haghtalab, B. Mokhtarani and G. Maurer, *J. Chem. Eng. Data*, **48**, 1170 (2003).
40. B. Perez, L. P. Malpiedi, G. Tubío, B. Nerli and P. A. P. Filho, *J. Chem. Thermodyn.*, **56**, 136 (2013).
41. M. Pirdashti. K. Movagharnejad, P. Mobalegholeslam, S. Curteanu and F. Leon, *J. Mol. Liq.*, **223**, 903 (2016).
42. K. S. Pitzer, *J. Phys. Chem.*, **77**, 268 (1973).
43. K. S. Pitzer, *J. Am. Chem. Soc.*, **102**, 2902 (1980).
44. J. M. Simonson and K. S. Pitzer, *J. Phys. Chem.*, **90**, 3005 (1986).
45. H. R. Radfarnia, G. M. Kontogeorgis, C. Ghotbi and V. Taghikhani, *Fluid Phase Equilib.*, **257**, 63 (2007).
46. G. R. Pazuki, V. Taghikhani and M. Vossoughi, *J. Ind. Eng. Chem.*, **48**, 4109 (2009).
47. J. C. Merchuk, B. A. Andrews and J. A. Asenjo, *J. Chromatogr. B.*, **711**, 258 (1998).
48. T. S. Porto, P. A. Pessôa-Filho, B. B. Neto, J. L. L. Filho, A. Converti, A. L. F. Porto and A. P. Jr, *J. Ind. Microbiol. Biotechnol.*, **34**, 547 (2007).
49. M.-K. Shahbazinasab and F. Rahimpour, *J. Chem. Eng. Data*, **57**, 1867 (2012).
50. A. R. D. Costa, J. S. D. R. Coimbrab, L. A. Ferreirac, J. C. Marcos, I. J. B. Santos, D. A. Marleny, M. D. A. Saldaña and J. A. C. *Food Bioprod. Process.*, **95**, 118 (2015).
51. M. Perumalsamy and T. Murugesan, *J. Chem. Eng. Data*, **54**, 1359 (2009).
52. S. M. Waziri, B. F. Abu-Sharkh and S. A. Ali, *Fluid Phase Equilib.*, **205**, 275 (2003).
53. R. N. Goldberg, *J. Phys. Chem. Ref. Data*, **10**, 671 (1981).